AN ABSTRACT OF THE THESIS OF

Yee Kit Leung for the degree Doctor of Philosophy

in Physics presented on June 16, 1975.

Title: ATOMIC EJECTION IN THE SINGLE CRYSTAL SPUTTERING OF NICKEL WITH 40-600 eV ARGON IONS

Abstract approved: Redacted for Privacy

James J. Brady

A three-stage, differentially pumped ion accelerator is used to produce low energy argon ions, which in turn, are used to bombard the surfaces of plane nickel single crystals. Nickel atoms ejected from the crystals are counted using the radioactive tracing method. From the analysis of the angular distributions of ejected atoms, the study of low energy single crystal sputtering is made possible.

The experimental procedure consisted of pumping down the accelerator to a pressure of 10^{-9} torr, outgassing the target by electron bombardment, generating a well-defined and singly ionized argon ion beam, and bombarding the target with ions for a time which is shorter than that required for gases to form a monolayer on the target surface at the existing residual partial pressure of absorbable gases.

Three targets, consisting of Ni^{63} being elcctroplated on the surfaces of two (110) and one (111) nickel crystals respectively, were used in this work. Each target was bombarded with 40-600 eV argon ions at normal incidence except one of the (110)

crystals which was mounted so that its surface normal made an angle of 20^{o} with respect to the incident ion beam. Nickel atoms ejected from the target were collected on a thin molybdenum foil. Immediately after each bombardment, the collector foil was cut into narrow strips, and the residual radioactivity of each strip was analyzed by placing it under a thin end-window G-M counter.

The angular distributions of nickel atoms ejected from the crystals were found to peak at directions corresponding to the close-packed crystal directions. The atomic intensity of each peak increased as the ion energy increased while its half-width remained about 8.5^{o}. These results indicate that at low energy ion bombardment atoms are ejected intensely around the close-packed direction from a single crystal and focused collisions may indeed narrow the distribution of the ejected atoms around this direction.

The sputtering yield curves for nickel atoms ejected along the [110] direction from a (110) and a (111) nickel crystals showed that the atomic ejection process was affected by the structure and atomic binding of the crystal surface and by the ion energy. At the same ion energy, the [110] sputtering yield obtained from a (110) crystal was higher than that from a (111) crystal.

For ejecting nickel atoms with low energy argon ions along a close-packed crystallographic direction, the most probable threshold energy for a (110) nickel was found to be 10 eV. For a (111) nickel crystal, the threshold appeared to have a value of about 15 eV. These results indicate that the surface binding energy may be a dominant factor in the atomic ejection process because the binding energy in a (111) nickel crystal is higher than that in a (110) nickel crystal. The experimental thresholds are higher than the threshold values predicted by Harrison-Magnuson's theory. This may indicate that the atomic ejection process is a complicated event. Further investigations, both experimental and theoretical, are desired in order to explain the ejection phenomenon near the threshold and to claim the final value of threshold energy.

Atomic ejection in the single crystal sputtering of nickel with 40 – 600 eV argon ions

by

Yee Kit Leung

A THESIS

submitted to

Oregon State University

in partial fulfillment of
the requirements for the
degree of

Doctor of Philosophy

Commencement June 1976

APPROVED:

Redacted for Privacy

Professor of Department of Physics

Redacted for Privacy

Chairman of Department of Physics

Redacted for Privacy

Dean of Graduate School

Date thesis is presented June 16, 1975

Typed by Margaret Chang for Yee Kit Leung

ACKNOWLEDGEMENT

I wish to thank (1) my major professor, Dr. James J. Brady for suggesting the problem and his support and interest in this work, (2) Mr. Robert McCune of the Bureau of Mines, Albany, Oregon for doing the x-ray diffraction analysis of the nickel crystals and helping to prepare the stereographic projections.

TABLE OF CONTENTS

LIST OF ILLUSTRATIONS

LIST OF TABLES

ATOMIC EJECTION IN THE SINGLE CRYSTAL SPUTTERING OF NICKEL WITH 40 - 600 eV ARGON IONS

I. INTRODUCTION

A. Definition of Sputtering

The ejection of atoms from a target as a result of bombardment with particles is called sputtering. This phenomenon was first observed by Grove (1852) over a century ago. The material ejected from polycrystalline metal was found to be isotropically distributed. Extensive study of sputtering was not carried out till the last decade after Wehner (1955) discovered that atoms were preferentially ejected from a single crystal in directions corresponding to low-index crystallographic directions of that crystal.

Sputtering experiments deal mostly with the measurements of the sputtering yield, which is defined as the average number of sputtered atoms per incident particle, the dependence of sputtering yield on the energy of the bombarding particles, and the angular distribution and energy of the atoms sputtered. Other interests in sputtering experiments are the effects on sputtering yield due to the variation of incident angle, i.e. the angle between the direction of the bombarding particle and the surface normal of the target, due to the mass of the bombarding particle and due to the target temperature. Sputtering experiments have

been done on amorphous target, polycrystalline and single crystals, in different forms of geometry, e.g. backward sputtering from plane and spherical targets; transmission sputtering of thin foils.

B. Experimental Requirements for Study of Sputtering

The following requirements, listed by Pleshivtsev (1964), must be satisfied by the sputtering experiments:

(1) The target must be annealed and outgassed in a vacuum, and its purity must be determined. It may be necessary to know the microstructure, the degree of roughness and hardness of the target surface, and the way in which it was processed. In order to make sure that the speed of eliminating the contamination due to the films that frequently form on targets under the influence of ion irradiation in the presence of residual gases exceeds the speed of formation of the films, the following condition must be satisfied:

$$6.25\times10^{18} sj \gg 3.5\times10^{20} pk$$

where j is the flux density of singly-charged ions at the target surface in amp/cm^2, 6.25×10^{18} is the number of ions incident on 1 cm^2 of the sample in one second when the ion density is 1 amp/cm^2, s is the sputtering coefficient for the contaminant film in atoms/ion, p is the pressure of residual gas molecules and in torr, 3.5×10^{20} is the number of molecules of nitrogen and oxygen incident on 1 cm^2 of the

sample surface per second at a pressure of 1 torr, and k is the probability for adhesion of gas molecules upon impact with the target surface.

(2) Ion beam used for bombarding a sample should have a minimal energy dispersion (1-5%) and should not contain foreign ions. The convergence or divergence of the ion beam must also be minimal ($1-3^{0}$).

(3) The total number of sputtered particles must be measured with an accuracy of 1-5%. Sputtered particles should not be permitted to return to the target, and if sputtered-particle collectors are used, it is necessary to know the number and energy of the reflected ions and atoms and be sure that they do not cause appreciable sputtering of the collector or the mass that is deposited on it.

C. Purpose of the Study

A large number of experimental results of medium and high energy sputtering, i.e. sputtering by particles with energy higher than 1 keV has been accumulated. Theoretical discussions in understanding these sputtering phenomena have been increasingly successful. In recent theories, the random collision cascade is frequently applied to explain the main feature of the atomic ejection process. The cascades of moving target atoms generated as a result of the multiple collision induced by the bombarding particles cause the ejection of target atoms. Sigmund (1969)

has proposed a theoretical model of sputtering yield of amorphous and polycrystalline targets based on the collisions characterized by the power approximation of the Thomas-Fermi cross section to quite accurately reproduce the experimental sputtering yields. The theory of sputtering yield of solid targets using a power potential law by Kanaya and his group (1973) also gives results in good agreement with experiment. In single crystal sputtering, the regular lattice structure apparently affects the atomic ejection process. Nelson et al. (1962) applied Silsbee's focused collision sequences to explain the anisotropic ejection that atoms received energy from the primary collisions at several lattice distances beneath the target surface caused the ejection of the surface atoms via collision sequences along the close-packed crystallographic directions of the crystal. Onderdelinden (1966) suggested that channeling of the incident ions had influence on the anisotrophy of the single crystal sputtering.

When the incident particle energy is reduced below 1 keV, the energy exchange between particles in the target will occur nearer to its surface hence fewer atomic collisions will be involved in the ejection process. At certain limit of incident particle energy, only those target atoms which experience the most energetically efficient collisions and receive sufficient energy can overcome the surface binding energy of the target and be ejected. Further reducing the incident particle energy will not induce any ejection of target atoms. This limiting energy

is called the threshold energy of sputtering for that certain sample. Once this energy is determined, information related to the atomic collision in the ejection process, to the surface binding energy and structure of the target, can be derived. The study of low energy sputtering, i.e. sputtering by particles with energy less than 1 keV, will help to understand the insight of collision phenomenon near the target surface and to develop and improve getter-ion pumps, ion microscopes and techniques like ion beam drilling, since their operations depend on the sputtering mechanism.

Interest in single crystal sputtering has recently increased because it is a phenomenon involved in many interesting atomic collision effects and can be used to identify mechanisms present in sputtering of materials.

The objective of this work was to study the angular distributions of nickel atoms ejected backwardly from plane nickel single crystals as a result of argon ion bombardment with energy less than 600 eV. From the analysis of angular distributions obtained in experiments, atomic ejection mechanism under bombardment with low energy ion was investigated, and then directional sputtering yields versus ion energy from each crystal were evaluated, and finally the threshold energies of sputtering for the crystals were determined.

The apparatus and procedure used in the experimental work will be described in chapter two, experimental results will be

discussed in chapter three, theoretical developments in low energy single crystal sputtering will be summarized in chapter four, and conclusions will be presented in chapter five.

II. EXPERIMENTAL

A. Apparatus

The experimental arrangement employed in this work is the one constructed by Cuderman (1968) in his study of low energy polycrystalline nickel sputtering. It consists mainly of an experimental tube which is shown in Figure 1 for producing an ion beam and a pump system.

The experimental tube is a linear, three-stage, differentially pumped glass tube, housing a Nier-type ion source and an extracting electric lens system (Stage I), accelerating or decelerating electric lens system (Stage II), and a target-collector assembly (Stage III). The assembly, a movable unit which can be inserted into or be withdrawn from the tube through the tube end, has a target support, an outgassing chamber and a collector support. The collector support is a steel cylinder of 24 mm i.d. by 18.3 mm wide by 0.75 mm thick and has two slits: a front entrance slit of 3.2 mm wide by 9.5 mm long for communicating with Stage II and allowing ions to pass through and hit the target which is mounted such that its surface to be bombarded is at the center of the collector support and faces the entrance slit; a rear slit of 6 mm wide by 12 mm long through which the target can be withdrawn into the outgassing chamber for outgassing, slid back into its position in order that it may be bombarded and withdrawn afterwards. The long sides of both slits

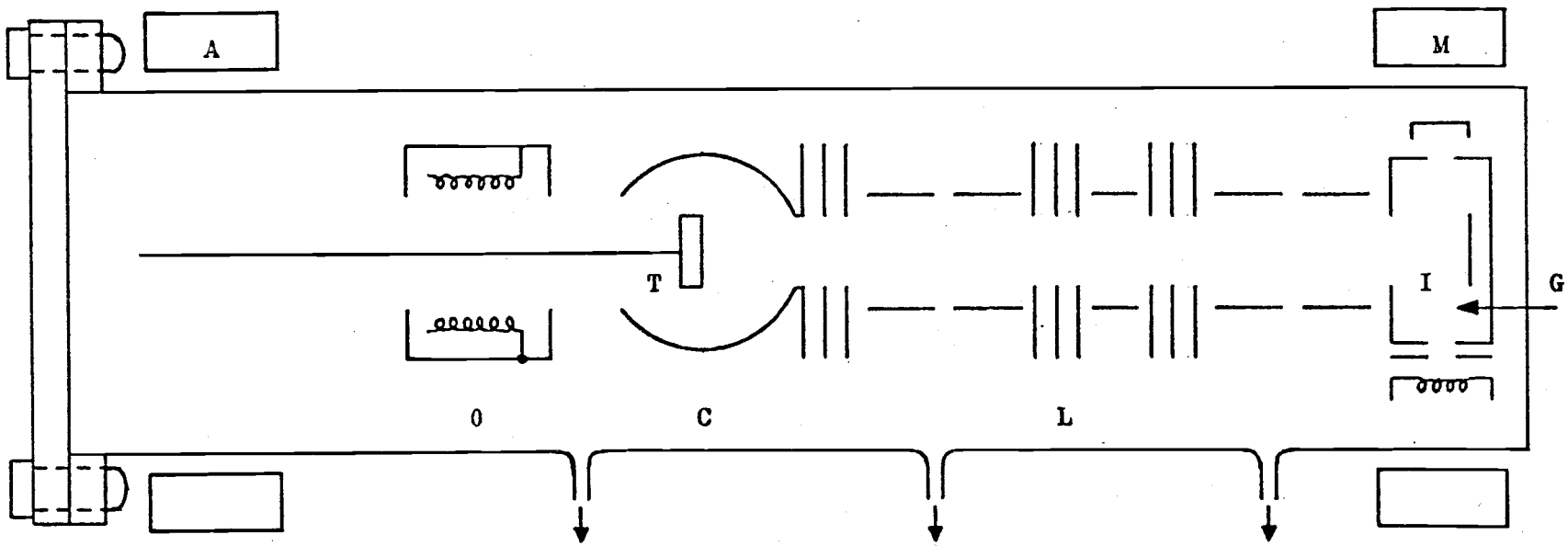

Figure 1. A schematic of the experimental tube
(A) Activating magnet; (C) Collector support;
(G) Argon gas; (I) Ion chamber;
(M) Collimating magnet;
(L) Electric lens system;
(O) Outgassing chamber; (T) Target.

are oriented parallel to the axis of the cylinder.

Ultra high purity argon used in the experiment was purchased from Union Carbide Corporation. The gas is introduced into the experimental tube through a gas-line which is connected to the tube through a Granville-Phillips ultra high vacuum valve which is closed all the time except during introducing argon gas into the tube for ion production. The gas-line is connected to a separate pump system through a valve.

Singly ionized argon ions, produced in the ion chamber using an electron impact method, are extracted, accelerated or decelerated, and finally focused on hitting the target surface. The ions are monoenergetic and in the energy range from a few eV to more than 1 keV, depending on the requirement of the experiment, with an energy spread such that 98% of the ions, at a given energy, are within ± 0.4% of the average energy.

A Varian conflat flange was installed at the tube end near Stage III such that the tube can be opened and closed without cracking the glass. Electric wiring was improved over the original Cuderman arrangement. Controls were added to all trap ovens, diffusion pump heaters and ion chamber filament such that whenever the cooling water to the diffusion pumps was off, simultaneously all the ovens and diffusion pump heaters would be switched off and the ion chamber filament would be disconnected from its batteries during bombardment. A switching circuit was added to the target outgassing circuit to provide on-off pulsing out-

gassing.

B. Target Preparation

Three plane nickel single crystals, with cross section of 3.2 mm by 9.6 mm and thickness of 9.6 mm, labelled as crystal A, B and C respectively, were used as targets. They were grown by Aremco Products, Inc., using RF-EB float method, with purity of 99.99%, and supposed to have orientation (110), (111) and (111) respectively.

Because small amounts of sputtered material were expected, a radioactive tracing method was used to detect the nickel atoms ejected from the crystal after each bombardment. Usually this method involves either a radioactive target or activating the material deposited on a collector foil by neutron bombardment. The first manner was chosen in this work.

The crystals purchased were not radioactive. In order to have them fitted for the experiment, the face of each crystal to be bombarded was electroplated in a dilute solution of Ni^{63} isotope, a beta emitter of half-life of 92 years and mean energy of 67 keV, in a chemical form of $NiCl_2$ in 0.5M HCl. The isotope was purchased from New England Nuclear, with a specific activity of 12.10 mCi/mg. Verma and Wilman (1971) have shown that nickel film electrodeposited on a copper crystal surface has the same structure and smoothness as its substrate, up to a plating current density of 600 mA/cm^2. Each nickel crystal was electropo-

lished and rinsed with distilled water, electroplated with a current density of about 1 mA/cm^2 for 40 minutes, then rinsed with a plentiful supply of distilled water. Assuming the current efficiency during the plating to be 100%, the Ni-63 film on each crystal surface had a thickness of the order of 2000 monolayers.

Thin molybdenum foil, of thickness of 0.125 mm, was used to collect the sputtered atoms. Each foil was cut to the size of the inner surface of the collector support cylinder, about 17 mm by 66 mm, with a rectangular hole of 9.6 mm by 3.2 mm at its center, and was clipped to the inner surface of the cylinder such that its hole coincided with the entrance slit of the latter prior to each experiment.

C. Experimental Procedure

After mounting a crystal and a collector foil on their respective supports, the target-collector assembly was carefully inserted into the experimental tube and the conflat flange was tightened after connecting the electrodes in the assembly to the lead-throughs in Stage III of the tube. The system was pumped down with three mercury diffusion pumps, which were connected to the respective stages of the experimental tube, backed up with forepumps to a pressure of about 10^{-6} torr. The main bakeout oven was lowered over the experimental tube to heat it to a temperature of $150^{\circ}C$ before removing the three high vacuum cold trap dewars, the tube and the high vacuum cold traps were then baked

out at 200°C for 20 hours. The trap ovens were then shut off and removed when they reached a temperature of about 100°C, and the cold traps were submerged in liquid nitrogen after they cooled to room temperature. The bakeout cycle was completed after the main oven was switched off and removed when the experimental tube cooled down to room temperature. The system pressure was reduced to 10^{-9} torr about 20 hours after the completion of bakeout. The gas-line was also evacuated with its own pump system at the same time, to a pressure of 10^{-4} torr, and was heated at a temperature of 200°C for outgassing.

Before the ion bombardment, a series of outgassing procedures was carried out. Firstly, by biasing the filament negative at 105 volts and the collector positive at 48 volts in the ion chamber, the filament was outgassed with a heating current of 2.8 amperes until the ion chamber pressure during the outgassing returned to its original reading. The electron current arriving at the collector was about 0.2 mA and was collimated by means of an external permanent magnet. Secondly, the crystal was drawn into the outgassing chamber in the target-collector assembly by means of an external magnet, then biased positive at 150 volts with respect to the filament in the outgassing chamber and bombarded with electrons on its four sides at a temperature of 1300°C for about two minutes. This outgassing procedure was repeated until the Stage III pressure during a bombarding interval remained the same as it was just prior to the outgassing.

Upon the completion of outgassing, the gas-line was purged with argon gas then pumped out to 10^{-4} torr. This purging procedure was repeated about 20 times to insure that the argon purity during the ion bombardment was maintained. The gas-line was then disconnected from its pump system by closing the valve between them and let in argon gas.

Using a torque wrench to slowly open the Granville-Phillips valve, argon gas was introduced into the experimental tube through the gas-line until Stage III pressure reached 10^{-7} torr, this also resulted in a pressure of 10^{-5} torr in the ion chamber. An ion beam of $5.0 \times 10^{-10} \pm 0.5 \times 10^{-10}$ amp was then turned on and focused onto the target surface for a bombardment of 20 min.

At the end of the bombardment, the Granville-Phillips valve was shut off. When the system pressure returned to 10^{-9} torr, ion chamber filament, power supplies and the diffusion pump heaters were switched off. The high vacuum cold trap dewars were removed when the diffusion pumps cooled to room temperature. The forepump cold trap dewars were removed when the high vacuum cold traps returned to room temperature.

The experimental tube was opened to air after warming the forepump cold traps to room temperature and shutting off the forepumps. Opening the conflat flange, the target-collector assembly was carefully removed from the tube. The collector foil was unclipped from its support, flattened and transferred on an adhesive plastic.

The experiment was repeated with different ion energies for the same crystal. The same procedure was then carried over to the other two crystals respectively.

Immediately after each experimental run, the collector foil was carefully cut into strips of preset size, 1.257 ± 0.109 mm wide by 17 mm long. Following the cutting, each strip was placed a few mm under a 1.4 mg/cm^2 G.M. end-window counter which was shielded in a lead chamber of thickness of 5 cm, and the residual radioactivity of the strip was determined at a background counting rate of 830 cph (counts per hour), for a period of at least one hour.

III. EXPERIMENTAL RESULTS

A. General Nature of the Experimental Results

The first aim of the experiment was to investigate the atomic intensity profiles of ejection patterns condensed on the collector foils, from each crystal separately, at different ion energies. The major features of the angular distributions of nickels atoms deposited on the collector foils are graphically illustrated on Figures 2, 4 and 7, for crystals A, B and C respectively, in terms of β-particle counts per hour above the background activity, as a function of ejection angle, i.e. the mean angle subtended by each strip of the collector foil relative to the ion beam.

In general, Figure 2 shows prominent peaks at angles of a few degrees with respect to the ion beam, and relatively small peaks at angles between 30^{o} and 60^{o}; Figure 4 shows two sets of asymmetric peaks at angles of 18^{o} and -22^{o}; while Figure 7 shows two sets of peaks at angles between 10^{o} and 50^{o}, and between -10^{o} and -40^{o}. Note that for crystal C, the ion bombardments were performed in such a way that the crystal was tilted at an angle of 20^{o} with respect to the ion beam, while for the other two crystals, the ions bombarded their surfaces perpendicularly. Also the faces of the crystals exposed to the ion beam were at 2 mm in front of the center of the collector support during the bombardment.

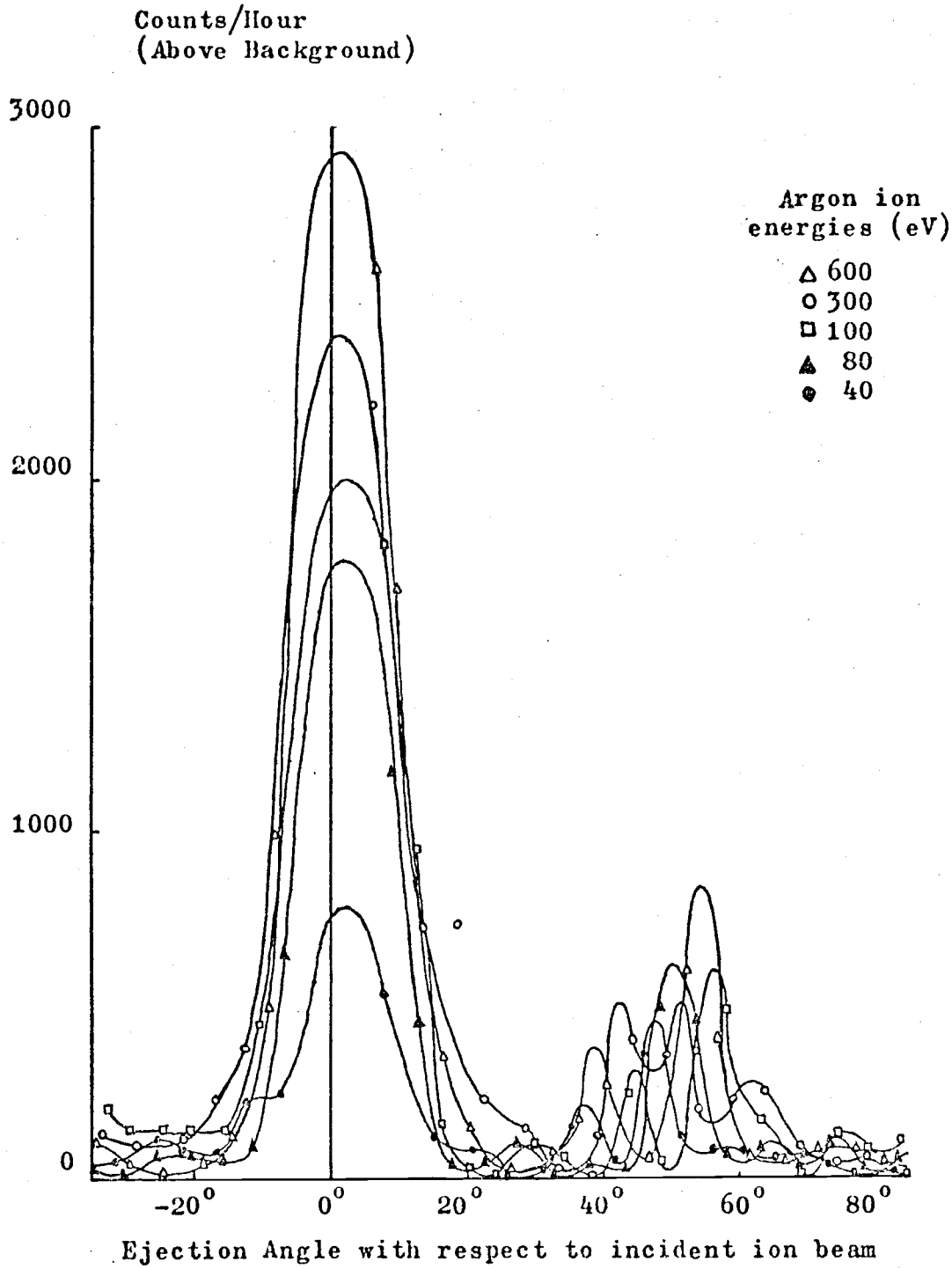

Figure 2. Angular distribution of nickel atoms ejected from crystal A by normally incident argon ions, as a function of bombarding energy.

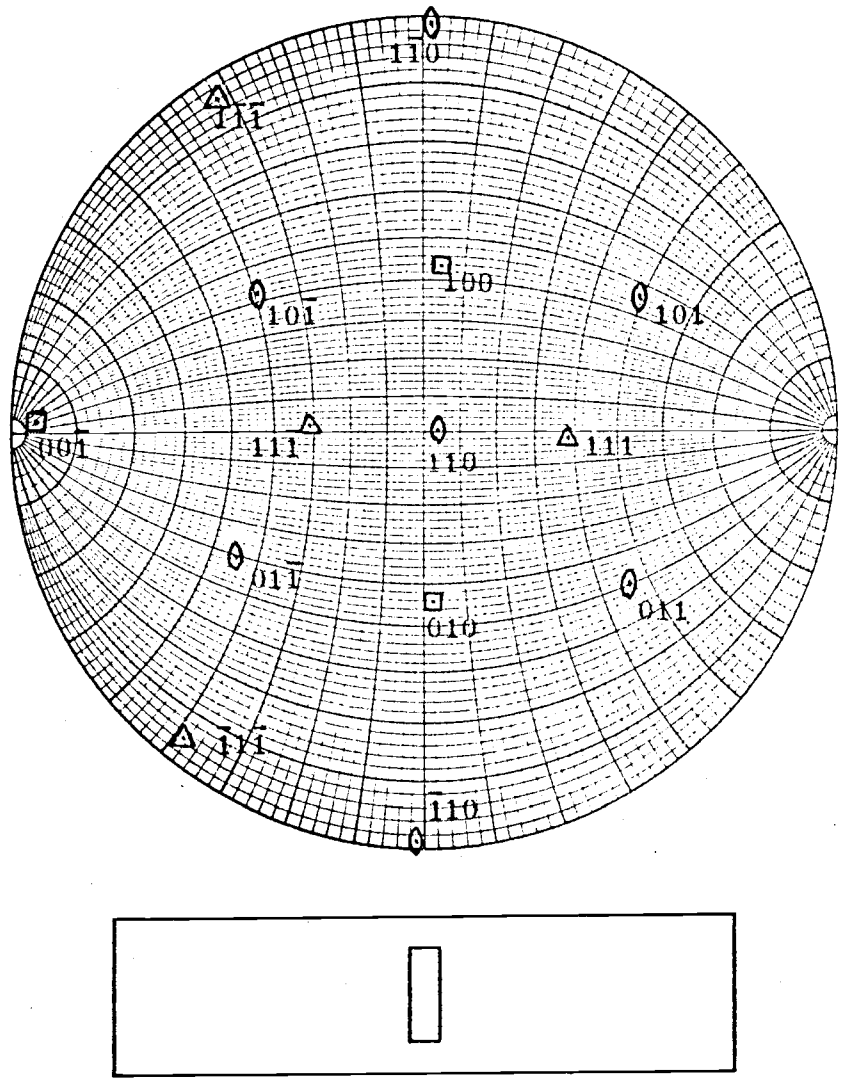

Figure 3. Stereogram of crystal A.

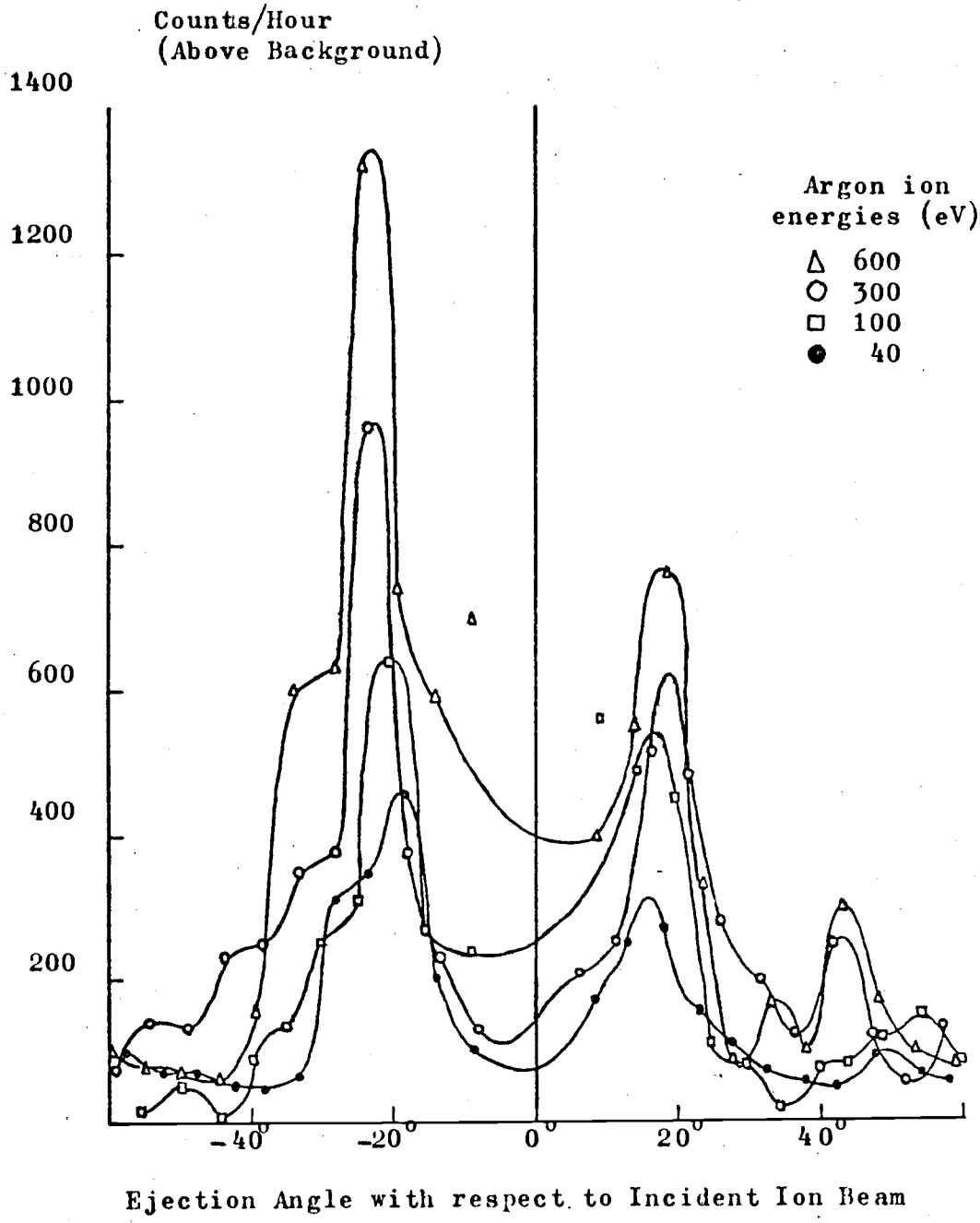

Figure 4. Angular distribution of nickel atoms ejected from crystal B by normally incident argon ions, as a function of bombarding energy.

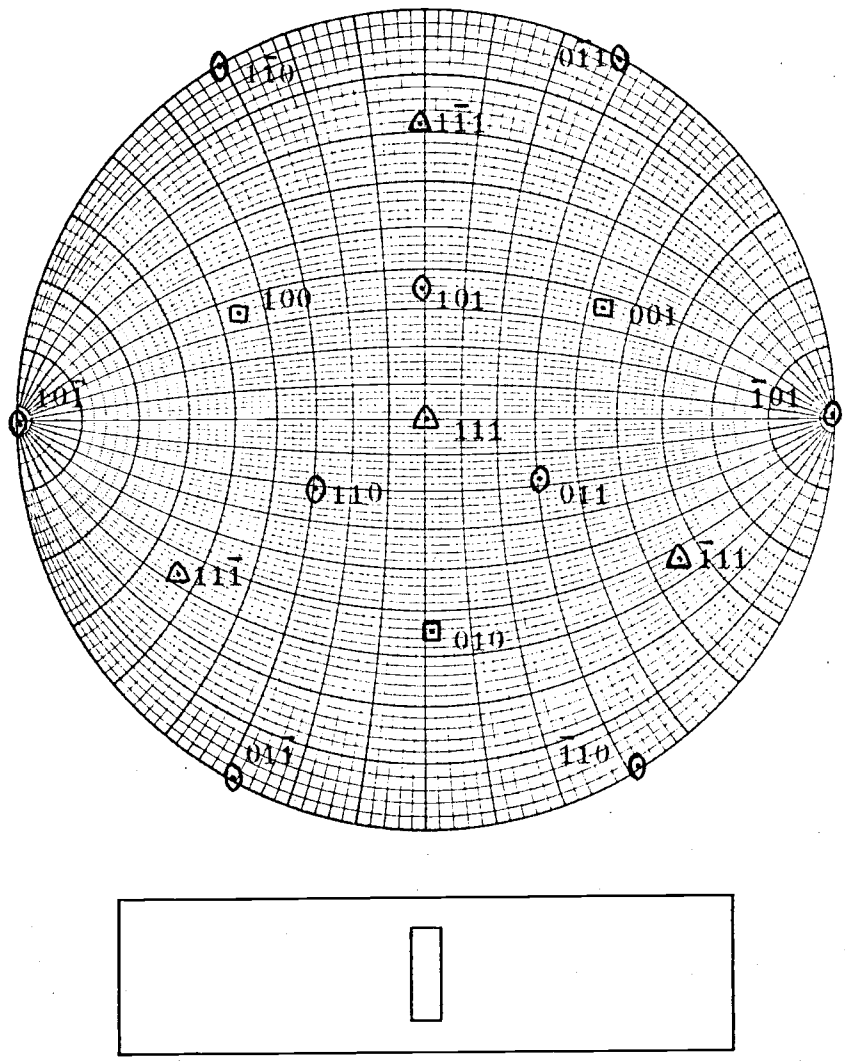

Figure 5. Stereogram of crystal B.

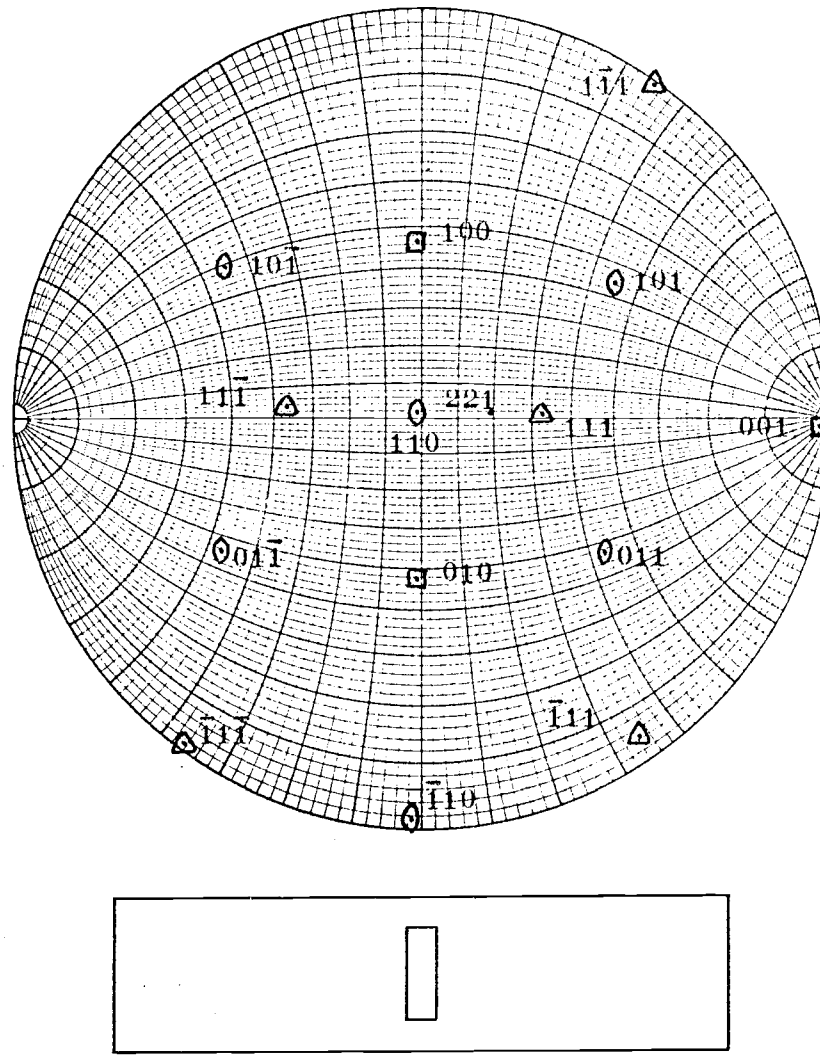

Figure 6. Stereogram of crystal C.

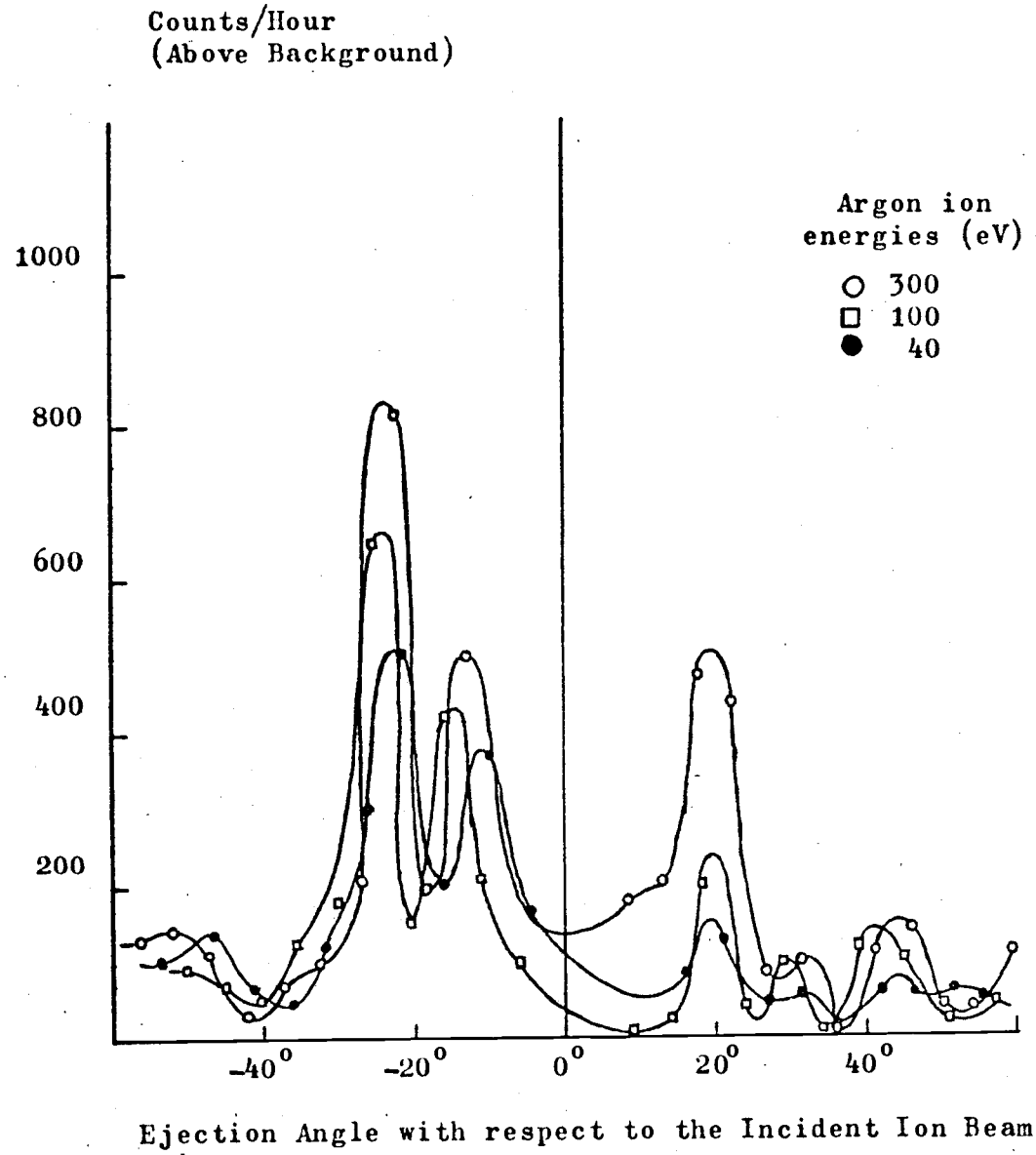

Figure 7. Angular distribution of nickel atoms ejected from crystal C, inclined at 20° to the incident argon ion beam, as a function of bombarding energy.

B. Interpretation of the Angular Distribution Patterns

The distribution curves in Figure 2 clearly indicate that most of the nickel atoms were ejected backwardly from crystal A along a direction at a few degrees with respect to the ion beam, while ejection of atoms also took place along directions between 30^{o} and 60^{o}. If the epitaxy film grown on the crystal surface has an orientation as its substrate specified by the manufacturer, i.e. a (110) orientation, and since the [110] direction is just the surface normal of the crystal, then the appearence of the prominent peaks provides the evidence that nickel atoms are ejected easily along the [110] direction as a result of argon ion bombardment. The ejection of atoms at a few degrees away from the normal of the crystal surface may be explained by assuming either the crystal surface was not vertical to the ion beam during the bombardment or the surface plane of the crystal was not exactly a (110) plane. X-ray diffraction analysis was performed on the surface of crystal A to study its orientation. By positioning the crystal relative to a copper K_{α} radiation so that many of its crystallographic planes were oriented to obey Bragg's law and gave a diffracted x-ray beam which was detected by a scintillation counter. The results were plotted on a stereographic projection which is shown in Figure 3. The stereogram reveals that crystal A indeed has a (110) structure except that the (110) plane tilts at an angle of about 4^{o} with respect

to the crystal surface. Since the Ni-63 film on the crystal surface had the same structure as its substrate, the position of the prominent peaks explains such tilting. The smaller peaks are not the evidences of nickel atoms being ejected along any [100] direction as the stereogram shows that the [100] and [010] directions point along the long side of the crystal surface hence any nickel atoms ejected along these directions would not condense on the long side of the collector foil. Obviously these smaller peaks also belong to the category of the <110> spots, they are weaker because only part of the atoms ejected along these directions condensed on the collector foil and because the argon ion beam was directed near the [110] channel, the [101] and [011] ejections fell into a minimum, a result similar to that observed by Chadderton et al. (1972) from a (100) copper crystal, a result in accord with the prediction of Onderdelinden(1968).

In Figure 4, the two sets of peaks indicate that nickel atoms were ejected along the directions at angles of 18^{o} and -22^{o} from crystal B respectively, as a result of argon ion bombardment. According to the manufacturer, crystal B should be a (111) crystal. A stereogram of crystal B is shown in Figure 5 which reveals that the crystal surface exposed to the argon ion beam indeed almost has a perfect (111) orientation. The peaks thus represent the <110> and <101> spots and are again the evidences of nickel atoms being ejected along the close-packed directions, for this case, from a (111) crystal. Because the <110> and <101>

spots condensed on the collector foil were not lying on its center line, the peaks should appear closer to the ion beam, i.e. at angles smaller than 35.26^{o} which is the angle between a [110] and a [111] direction in a cubic crystal. The asymmetry of these two similar spots was due to the crystal being rotated 5^{o} about the ion beam direction. This rotation resulted in bringing the ⟨110⟩ spot closer to the center line of the collector foil to appear as a -22^{o} spot while moving the ⟨101⟩ spot further away to appear as a 18^{o} peak.

The only crystal surface left for identification is the one on crystal C. This crystal should be a (100) crystal, so should the structure of the Ni-63 film plated on it, but the stereogram of it shown in Figure 6 reveals a (110) orientation. Indeed the angular distribution of nickel atoms ejected from this crystal showed a similar pattern as the one obtained from crystal A. It can be concluded that crystal C is just another (110) crystal and was mishandled by the manufacturer while the crystal was cut or grown. In order to make use of this crystal, ion bombardment was done in such a way that the crystal was tilted at an angle of 20^{o} with respect to the ion beam. The angular distribution of nickel atoms ejected at three different ion energies are shown in Figure 7. The tilting of the crystal resulted in an ion bombardment being directed near the [221] direction of the crystal. The two sets of peaks at angles between -10^{o} and -40^{o}, and at

angles between 10^{o} and 30^{o} thus may indicate that nickel atoms were ejected along the [110], and [101] or [011] directions of the crystal respectively.

C. Analysis of the ⟨110⟩ Spot Patterns

The angular distribution of atoms ejected as a result of single crystal sputtering is usually expressed in terms of the variation of atomic intensity about a close-packed preferential direction. The ejection profiles have been observed for several metals, and they all show a distribution approximately Gaussian in the intense region except a smooth cutoff with an extended tail. In order to explain this departure, Endzheets et al. (1963) suggested that the anisotropic ejection was accomplished by an isotropic ejection due to the background sputtering from the ejection of atoms not at their normal lattice positions. Chapman and Kelly (1967) proposed that the ejection distribution was a result of the superposition of a preferential ejection distribution and a background ejection distribution, and the anisotropic ejection was assumed to be

$$S(\theta) = S(0)\ \exp\left(-\frac{\theta^2}{2\theta_w^2}\right)$$

where θ is the angle of ejection made with respect to the pre-

ferential direction. The ejection intensity along this direction $S(0)$ and the half-width θ_w of the distribution were adjusted to give the best fit to the experimentally measured ejection distribution. Distortion exists in the distribution pattern obtained in the sputtering experiment in which the atomic intensity is determined by the mass collected on either a hemi-cylindrical or a hemi-spherical foil. Hoffer (1974) suggested that, excluding condensable metal like copper, the incomplete nucleation during the condensation process of the ejected atoms on the collector foil might cause the distortion and make the ejection pattern to appear sharper than actually it should be.

The sources of distribution disturbance in this work might include: (1) geometric effect, e.g. the collector foil might not be in the exact form of a cylindrical surface during the depositing of material, (2) slicing effect, e.g. the cutting of collector foil into strips might remove certain amount of nickel atoms in the process, the narrower the strip, the finer the detail of the pattern, but the greater the disturbance.

In general, the height of the peak obtained in this work increases as ion energy increases although the exact relationship between them still requires further investigation. The half-widths of all peaks, regardless of the crystal structure, were found to be about 8.5° and independent of the ion energy, at least for argon ion energy up to 600 eV.

Comparing the shapes of the peaks, the following observa-

tions are obtained:

(1) The prominent ⟨110⟩ peaks obtained from the (110) crystal appear sharper than all other peaks.

(2) The peaks obtained from the (111) crystal show the appearance of a shoulder structure.

(3) The smaller peaks obtained from the (110) crystal are approximately asymmetric about 50^{o} with respect to the ion beam, while the two sets of peaks obtained from crystal C are asymmetric about 30^{o} and -16^{o} respectively.

The last two features are interesting because the development of a similar structure was also observed by Chadderton et al. (1972). In their 10-80 keV Ar^{+} ion bombarding a (100) copper crystal experiment, double peaks appeared at the ⟨101⟩ spot pattern when the incident ion beam was tilted at a few degrees away from the [001] channel and at the ⟨011⟩ and ⟨$\bar{1}$01⟩ spot patterns when the incident ion beam was directed at a few degrees away from the [101] channel.

Nelson (1971) has demonstrated that peak height of ⟨110⟩ spots in the ejection patterns from (100) surfaces of gold is dependent on the mass of the impinging ion, the greater the mass, the higher the ratio of the random to preferential ejection. He proposed that the variation of the ratio with ion mass and energy was due to the changes in the proportion of the randomized cascade and in the depth of the cascade below the target surface. Chadderton and his group suggested that the origin of the spot

structure might depend on the cascade structure. When the ion beam is "crudely" split into channelled and random components at the crystal surface, cascades are generated both immediately at the surface itself due to the primary collisions there and in the bulk of the crystal following dechanneling. As the angle between the ion beam and the crystal surface increases, the fraction of cascades at the geometrical surface remains essentially the same while the cascades inside the crystal are brought closer to the surface due to the increase of dechanneling probability. The latter make an additional contribution to the ejection of target atoms, both in and out of the ejection direction. This explanation seems applicable to the result of this work. The appearance of a shoulder structure in the peaks obtained from the (111) crystal provides the sign of a double peak in its early developing stage because the argon ion beam was actually incident at about half of a degree away from the [111] axis in the crystal. The double peak becomes evident from the ejection of nickel atoms along the [101] or [011] direction in the (110) crystal when the ion beam bombarded the crystal along a direction at about 4^{o} away from the [110] channel and from that along the [110], [101] or [011] directions in the crystal C when the ion beam was directed along the [221] channel of the crystal. It can be concluded that actually the peaks in the angular distributions obtained from (111) crystal should be asymmetric about -27^{o} and 26^{o} respectively, i.e. the angles of [110] and [011]

directions make with respect to the ion beam along the center line of the collector foil. Similarily the double peaks appeared in the angular distributions of nickel atoms ejected from the (110) crystal are asymmetric about the [101] or [011] direction because they make an angle of 50^{o} with respect to the ion beam along the center line of the collector foil, while the two sets of double peaks obtained from crystal C should be asymmetric about the [101] and [011] direction respectively because they are at angles of -16^{o} and 30^{o} away from the ion beam direction respectively.

The sharpness of the prominent <110> peaks obtained from the (110) crystal may indicate that focused collisions took place or at least affected the atomic ejection process.

Experimental half-widths of <110> peaks exist for Al ($\sim 10.5^{o}$), Cu($\sim 9^{o}$) and Au($\sim 6^{o}$) (Lenskjaer et al., 1974). Including nickel, all these metals have f.c.c. crystal structure. There is a tendency that the higher the atomic weight of the element, the narrower the half-width of the <110> peak. The same relationship is true between the focusing energy E_f^{110} and the half-width. This indicates that the half-width of the <110> spot pattern may depend on the focusing energy E_f^{110}, the atomic mass of the material, as well as on its surface binding energy.

D. [110] Sputtering Yield and Sputtering Threshold

The spot profiles obtained in the present radioactive counting technique can be made evident by an integration of the total number of nickel atoms into a solid angle defined by each strip of the collector foil, then the sputtering yield as a function of ion energy can be exaimined. Figure 8 shows two [110] sputtering yield curves, by plotting the peak counting rate versus the argon ion energy, for the (110) and (111) crystals respectively. At the same ion energy, the number of atoms ejected along the [110] direction from a (110) crystal is higher than that from a (111) crystal. This indicates that the binding energy of a crystal surface may be a dominant factor in the directional ejection process because the surface binding energy of a (111) nickel crystal is higher than that of a (110) nickel crystal. The sputtering yield also appears to be a sensitive function of the angle between the incident ion and the ejected atom. In general, both yield curves almost have the same shape.

The sputtering data of Stuart and Wehner (1962) and of Cuderman (1968), for sputtering of nickel by Ar^+ ions, are also shown in Figure 8 to permit comparison with the results of this work. Note that the 75° yield in Cuderman's data represents the ejection of nickel atoms along the [110] direction from a highly ordered polycrystalline nickel. The ordinate scale of Figure 8 was chosen such that the 200-eV yield of Stuart and Wehner and

the 75^{o} yield of Cuderman at 200 eV coincide with the present [110] yield for the (110) crystal at 200 eV.

At ion energies between 100 eV and 600 eV, the [110] sputtering yields obtained in this work increase with a slower rate than that at ion energies below 100 eV as the ion energy increases. This may indicate that a change in collision mechanism takes place at ion energy near 100 eV. The appearance of a knee structure in the yield curve at 100 eV was probably due to a rapid increase of the number of the focused collision sequences near the threshold and a reduced rate of such increase at ion energies higher than 100 eV.

The number of target atoms ejected from a target increases as the ion energy increases until the latter reaches a limit above which the number of atoms ejected will remain the same or reduce if the ion energy is further increased. Cuderman's yield curve shows a rapid saturation at ion energies above 300 eV. Such saturation, however, does not occur in the [110] yield curves of this work. On the other hand, at ion energies below 100 eV, the present yields decrease at a faster rate than that of Stuart and Wehner and of Cuderman as the ion energies decreases. Since the target used by Stuart and Wehner was polycrystalline nickel and that used by Cuderman was also polycrystalline nickel except that it had a highly ordered structure, while the targets used in this work were well-oriented single crystals, the channeling of incident ions and the ejection of target atoms along

the close-packed direction seem to increase the number of ejected near the threshold.

The experimental sputtering threshold is determined from the ion energy at which the sputtering yield is a minimum or zero. From Figure 8, the most probable threshold energy required to eject nickel atoms along a [110] direction from a (110) nickel crystal as a result of argon ion bombardment is found to be about 10 eV. Because of the statistical errors in measuring foil activities, the following limits have to be placed on the most probable value of the extrapolated threshold: $5\ \text{eV} < E_T < 15\ \text{eV}$. For a (111) nickel crystal, the threshold appeared to have a value of about 15 eV. Stuart and Wehner reported a 21-eV threshold for ejecting nickel atoms from polycrystalline nickel, and Cuderman's results indicated a threshold value between 18 eV and 25 eV for ejecting nickel atoms along the [110] direction from a highly ordered polycrystalline structure of nickel, as a result of bombardment with argon ions, while a threshold of 9 eV was obtained by Askerov and Sena (1969) in their experiment of bombarding polycrystalline nickel with low energy mercury ion. The sputtering threshold seems to depend on the binding energy and structure of the target surface, and the mass of the ion.

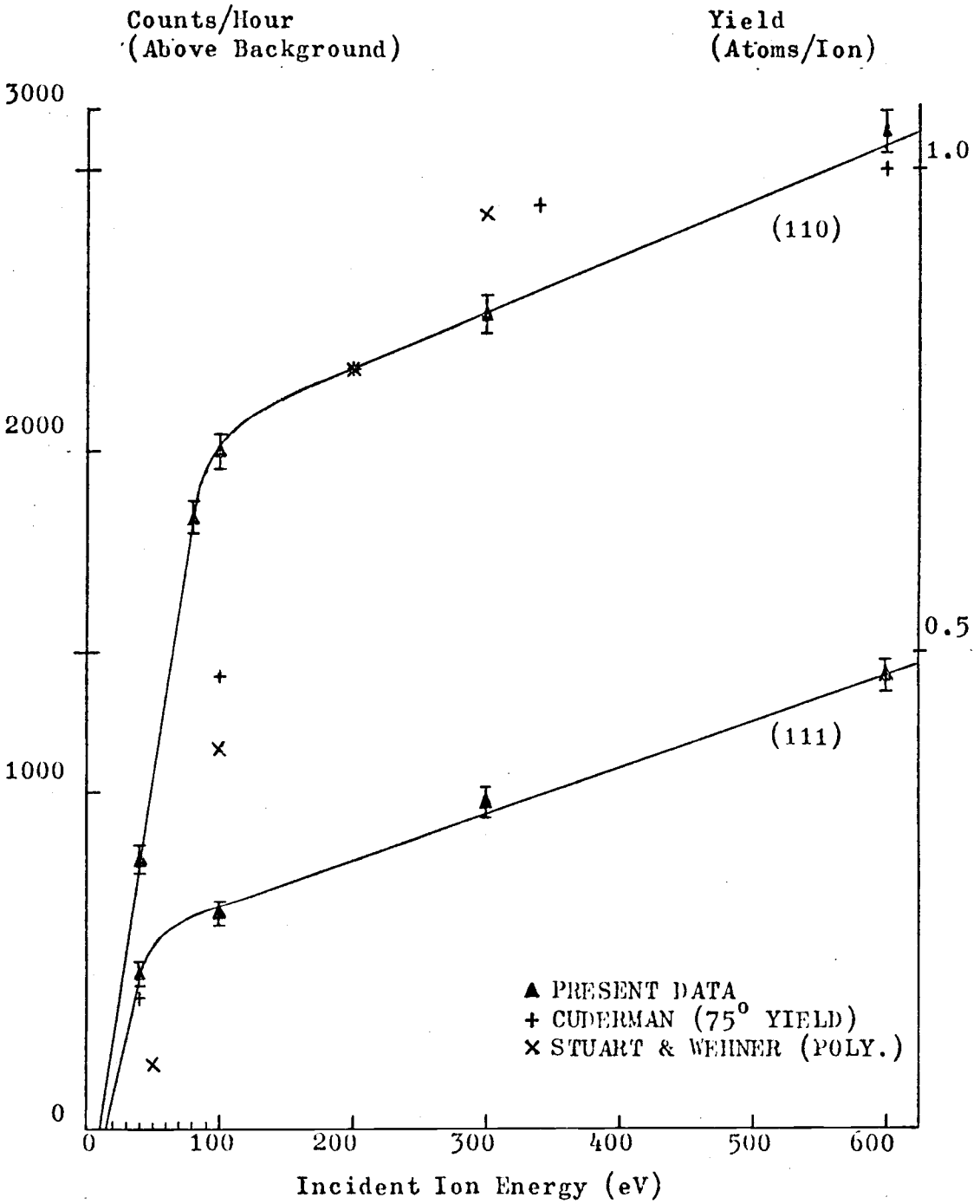

Figure 8. [110] sputtering yields for Ar^+ bombardment of (110) and (111) nickel crystals.

IV. THEORETICAL

A. General Discussion

When an ion hits the surface of a target, collision processes with the target atoms take place. The incoming ion collides with a target atom near the surface, it can displace the latter locally to form a vacancy-interstitial pair, or the collision would start a focused collision sequence which can result in damage to the target. The incoming particle thus can either penetrate into the target, depending on its initial energy, and finally be trapped inside the target, or scatter away from the target. The collision between the ion and the target atoms can also cause the ejection of target atoms from the target.

At low energy ion bombardment, the atomic ejection would be expected as a pure surface effect because the penetration of ions, especially the heavy ones, is generally small.

In the low energy region, the interatomic potential $V(r)$ is not well known because it varies rapidly with the distance r between the interacting partners. The Born-Mayer potential

$$V(r) = A \exp(-\frac{r}{a}) \qquad (1)$$

where r is the interatomic distance, A is a constant, and a is the screening radius, is often used to study the atomic collision and ejection phenomenon. The values of A and a are often fitted

empirically to one observed property, and then the potential function is used to determine other physical properties. Generally, the evaluations of these two constants by Abrahamson (1969), based on a Thomas-Fermi-Dirac (TFD) approximation, are thought to be applicable in this energy range of interest. Table I shows the values of the two constants for Au, Cu and Ni. In order to describe the collision process analytically, the two-body hard-sphere collision is usually employed because it is simple to handle. However this approximation is generally suspect at very low energies, and it also fails to reproduce certain effects, e.g. the replacement collision. A more realistic soft collision model is also often used to explain the collision process in this energy range.

B. Focused Collision Sequences (Focusons)

In treating the problems of sputtering and radiation damage of solids, Silsbee (1957) proposed that, by using a billiard ball collision model, a correlation between sucessive collisions being implied by the structure of a crystal could lead to the propagation of an energy pulse, or a sequence of collisions, along a close-packed line of atoms inside the crystal. His analysis was considerably extended by Leibfried (1958).

Consider a row of atoms, represented by spheres with radius R and interatomic distance d between two adjacent atomic centers in the row direction, if the n^{th} member of the row, with energy

TABLE I. PARAMETERS IN BORN-MAYER POTENTIAL FOR Cu, Au AND Ni

	Abrahamson		Anderson[#] and Sigmund		Empirical	
Metals	A(keV)	a(A)	A(keV)	a(A)	A(keV)	a(A)
Au	59.47	0.29	36.51	0.22	200.00	14.33[*]
Cu	13.92	0.28	8.12	0.22	22.50	13.00[**]
Ni	13.27	0.28	7.70	0.22		

TABLE II. FOCUSING ENERGIES E_f^{110} FOR Au, Cu and Ni

Collision	Metals	Abrahamson	Anderson & Sigmund	Empirical	Experiment
Hard-sphere (eV)	Au	770	102	310	170 ± 25[*]
	Cu	296	47	40	50 ± 10[##]
	Ni	313	53		
Soft (eV)	Au	386	49	137	
	Cu	154	23	31	
	Ni	164	25		

Anderson and Sigmund (1965)
Farmery and Thompson (1968)
* Thompson (1968)
** Gibson et al. (1960)

E_n, moves in a direction θ_n with respect to the row, as shown in Figure 9, and the initial velocity of the remaining atoms as they are struck makes sucessively smaller angles θ_{n+1}, θ_{n+2}, ... with respect to this row, then from triangle $00'0_1$, the following relations can be obtained:

$$\frac{\text{Sin } \theta_{n+1}}{\text{Sin } \theta_n} = \frac{h}{2R} \tag{2}$$

and

$$(2R)^2 = h^2 + d^2 - 2hd \text{ Cos } \theta_n \tag{3}$$

Solving h from Equation (3) results:

$$\frac{h}{2R} = \frac{d}{2R} \text{ Cos } \theta_n - \left\{1 - \left(\frac{d}{2R} \text{ Sin } \theta_n\right)^2\right\}^{\frac{1}{2}}.$$

Defining $\alpha = d/2R$, and using Equation (2), the relationship between the angle θ_{n+1} 0f the knocked on to the angle θ_n is found to be

$$\text{Sin } \theta_{n+1} = \text{Sin } \theta_n \left\{\alpha \text{ Cos } \theta_n - (1 - \alpha^2 \text{Sin}^2 \theta_n)^{\frac{1}{2}}\right\}. \tag{4}$$

Conservation of momentum and energy requires

$$v_n \text{Cos } \theta_n = v_n' \text{Cos } \theta_n' + v_{n+1} \text{Cos } \theta_{n+1}$$

$$v_n \text{Sin } \theta_n = v_n' \text{Sin } \theta_n' - v_{n+1} \text{Sin } \theta_{n+1}$$

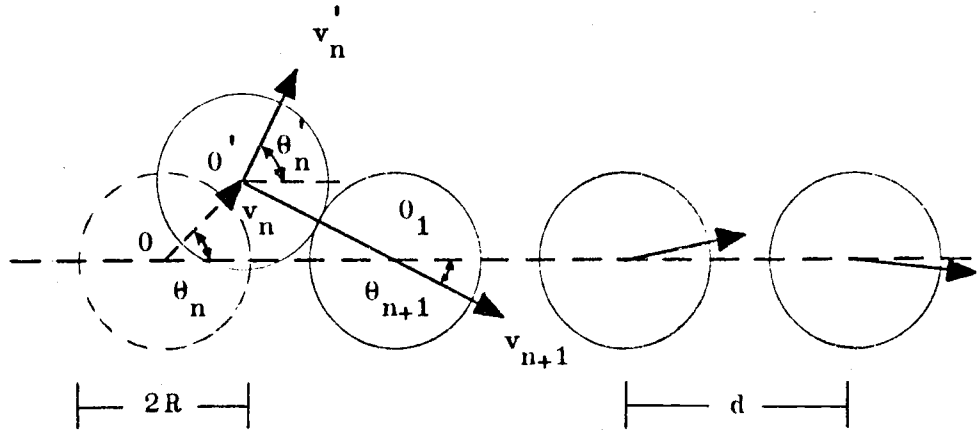

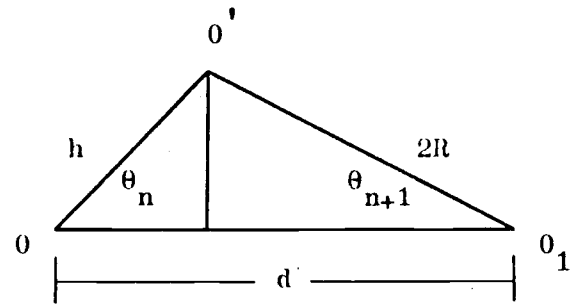

Figure 9. An illustration of focusing effect.

and

$$v_n^2 = v_n^{'} + v_{n+1}^2$$

where $v_n^{'}$ is the velocity of the incident atom and $\theta_n^{'}$ is its angle with respect to the row after the collision. Note that

$$\theta_n^{'} + \theta_{n+1} = \tfrac{1}{2}\pi .$$

The energy transferred in the collision is found to be

$$E_{n+1} = E_n \mathrm{Cos}^2(\theta_n + \theta_{n+1}). \tag{5}$$

Using Equation (4) and the following equation derived from it

$$\mathrm{Cos}\ \theta_{n+1} = \alpha \mathrm{Sin}^2\theta_n + (1 - \alpha^2 \mathrm{Sin}^2\theta_n)^{\frac{1}{2}} \mathrm{Cos}\ \theta_n , \tag{4'}$$

Equation (5) can be rewritten into

$$E_{n+1} = E_n(1 - \alpha^2 \mathrm{Sin}^2\theta_n). \tag{5'}$$

The interaction distance 2R can be determined from

$$E = 2V(2R) \tag{6}$$

where E is the kinetic energy of the moving atom.

When $d < 4R$ and $\theta_{n+1} \leq \theta_n$, the impulse will be focused into the row in successive collisions. A quantity used to describe the focusing action called the focusing parameter $f(E_n, \theta_n)$ is

defined as

$$f(E_n, \theta_n) = \frac{\theta_{n+1}}{\theta_n} \quad . \tag{7}$$

Focusing occurs when $f(E,\theta) \leq 1$. The maximum energy of an atom to start a focused collision is called the focusing energy E_f and at which the focusing parameter is equal to one.

In a f.c.c. crystal, the [110] direction has the smallest d, hence focused collision can be expected predominantly in this direction. The focusing energy E_f^{110} is determined from

$$E_f^{110} = 2V(\tfrac{1}{2}d^{110}). \tag{8}$$

For small angle scattering, the focusing parameter $f^{110}(E)$ is found to be independent of angle and given by

$$f^{110}(E) = \frac{d^{110}}{2R} - 1 \quad . \tag{9}$$

Duesing and Leibfried (1965) showed that the value of E_f^{110} determined from the focusing parameter based on the soft collision appeared to be in better agreement with experiment than that based on the hard-sphere collision, and that for small angle scattering the focusing parameter could be approximately expressed as

$$f^{110}(E) \sim \left(\frac{E}{E_f^{110}}\right)^m \tag{10}$$

with $0 \leq m \leq \frac{1}{2}$. A comparison between the theoretical and experimental values of E_f^{110} for Au, Cu and Ni is shown in Table II.

As soon as the momentum vectors are focused along the row direction, and if there is no energy loss, the focused collision chain would be infinitely long. However, the moving atom is perturbed by the potentials of atoms in the neighboring rows, at the moment of collision, the moving atom has already transferred a part of its kinetic energy into the potential energy with respect to an atom in a neighboring row. Other posibilities of energy loss can also exist, i.e. the atoms in the collision chain may not be perfectly in line as a result of their thermal vibrations. Nelson, Thompson and Montgomery (1962) have shown that the mean angle of deviation, as a result of thermal vibrations of atoms with respect to the row direction at target temperature T, is given by

$$\langle\theta\rangle^2 = \frac{3}{M_2 c d^{110} L(1+L)\,\eta\,\pi}\left\{1 - \frac{2}{1+L}\left[0.139 - 0.047\left(\frac{1-L}{1+L}\right)\right]\right\} \qquad (11)$$

at $T \ll \Theta_D$, or

$$\langle\theta\rangle^2 = \frac{12kT}{M_2 \hbar L(1+L)(\eta\, c\pi)^2}\left\{1 - \frac{1}{\eta(1-L)}\ln\left(\frac{2}{1+L}\right)\right\} \qquad (12)$$

at $T > \Theta_D$, with

$$L = \frac{2a}{d^{110}} \ln\left(\frac{E_f^{110}}{E}\right)$$

$$\eta = \left(\frac{6\sqrt{2}}{\pi}\right)^3$$

where Θ_D is the Debye temperature of the target, M_2 is the mass of a target atom, c is the speed of light, k is the Boltzmann's constant and E is the energy of a target atom to start a collision sequence. The Debye temperature for nickel is $379^{o}K$ (Paakkan, 1974).

The next nearest neighbor direction in a f.c.c. crystal is the [100] direction. Because d^{100} is so large, focusing can only occur as a result of the lenses formed by the surrounding four rows of atoms. This mechanism is called lens focusing (Nelson and Thompson, 1961). Any atom to start or to relay a collision sequence along the [100] direction has to pass through an atomic lens before it transfers its energy to the next atom in its row, hence the focusing energy for this direction is determined from the energy of the atom needed to pass through the potential barrier in the middle of the lens.

It is generally considered that single crystal sputtering is mainly a result of focused collision sequences in the target, directed either forwardly or backwardly, with sufficient energies to eject the surface atoms at the ends of the sequences. These collision sequences are started by the bombarding ions or by the

target atoms scattered through one or more than one non-focused collisions, hence the target atoms ejected are found to be distributed predominantly near the close-packed crystal direction where the focused collision sequences are expected.

Harrison et al. (1966) have performed computer simulations of high energy sputtering process and concluded that the ejection patterns observed in the sputtering experiments did not necessarily arise as a consequence of focusons and the magnitude of sputtering yield could be explained by the primary collision events taking place quite close to the crystal surface (SCC). However their calculations were produced under conditions at which focusons were not expected to be significant.

C. Analysis of Ejection Patterns

Atomic ejection patterns obtained from single crystal sputtering experiments show characteristic spots corresponding to the ejection of target atoms along certain close-packed crystal directions. Lehmann and Sigmund (1966) suggested that the appearance of spot patterns in single crystal sputtering could be explained by simply assuming the crystal surface to have a regular structure. Surface atoms could be ejected from a crystal when they received sufficient energy from the impinging particles to overcome the surface binding energy of the crystal. Since the energy distribution of these atoms was found to strongly peak at small energies, the atomic intensity of the spot pattern would have pronounced maxima in the crystal directions where atomic

ejection required a minimum of energy.

Two mechanisms of single crystal sputtering have been proposed:

(1) Close-neighbor sputtering.

Atoms in the uppermost surface layer of a crystal can be ejected very easily by means of a collision started by one of its close neighbors beneath the target surface.

(2) Assisting sputtering.

Atoms in layer just beneath the crystal surface have to penetrate more or less symmetric rings of surrounding atoms before being ejected. Ejection of these atoms can take place along the axis of an atomic ring. Because of the relatively high potential barriers, these ejection patterns can occur at several hundred eV bombarding ion energy.

A sketch of these two mechanisms is shown in Figure 10.

For random slowing-down of atoms within polycrystalline targets of Cu and Ni under bombardment with Ar^+ ions of 900 eV, the energy distribution of subsurface atoms can be approximately represented by

$$g(E_1) \sim \left(\frac{U}{E_1}\right)^2 \qquad (13)$$

(Oechsner, 1970) where E_1 is the energy of the subsurface atom and U is the surface binding energy of the target. Assuming that this isotropic energy distribution is also applicable to

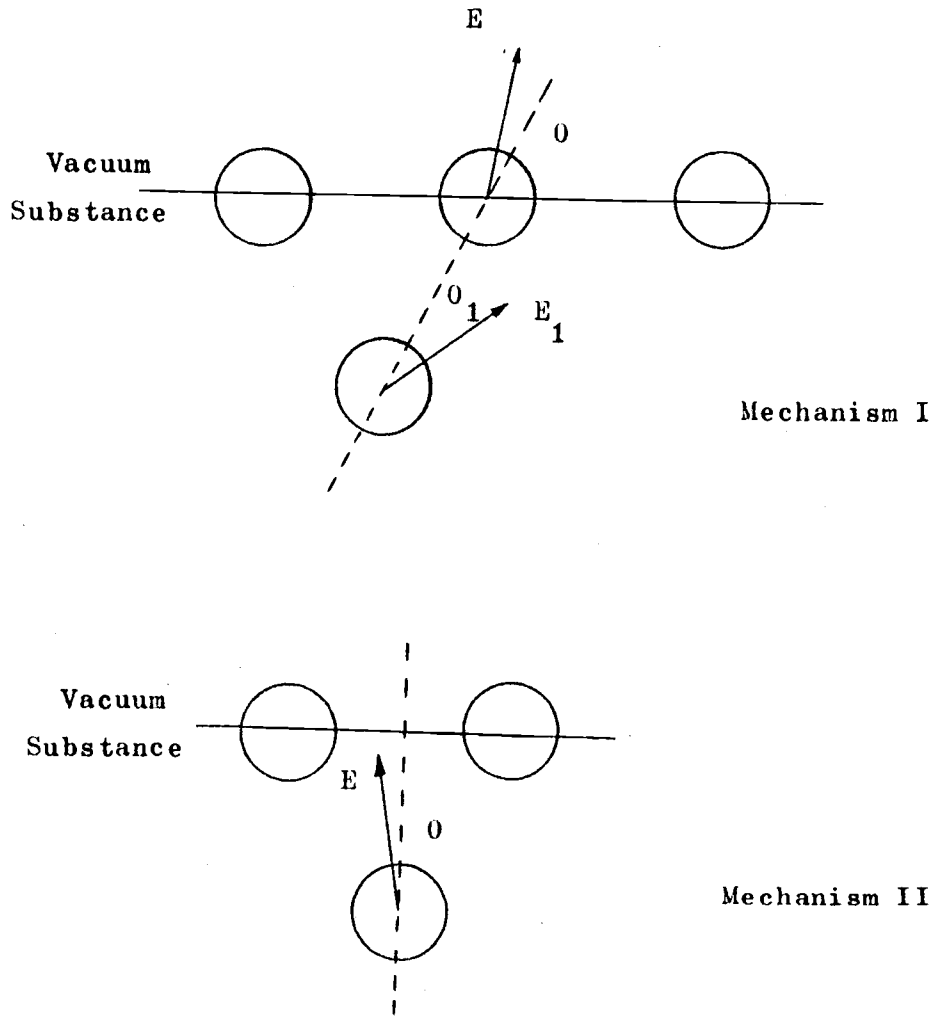

Figure 10. Lehmann-Sigmund single crystal sputtering mechanisms.

the subsurface atoms in a single crystal and that the scattering between a surface atom and one of its close neighbors in the crystal is expressed by

$$\theta = f(\theta_1, E_1)\theta_1$$

where θ and θ_1 are the angles of the surface atom and its close neighbor making with a close-packed direction of the crystal, the angular distribution of surface atoms sputtered around the considered direction, according to the close-neighbor sputtering of Lehmann and Sigmund's theory, is given by

$$S(\theta) \sim \int_w^\infty g(E_1) f^{-2}(E_1)\, dE_1$$

with

$$w = \frac{U}{\cos^2\left\{\left(1 + \frac{1}{f(U)}\right)\theta\right\}} \quad .$$

For small angles with respect to the ejection direction, the surface binding energy U can be assumed to be independent of angle θ. The focusing parameter, for Born-Mayer interaction and small angle scattering, can be approximately expressed by

$$f(E_1) \sim (E_1/E_f)^m, \qquad 0 \leq m \leq \tfrac{1}{2}$$

then

$$S(\theta) = S(0)\ \mathrm{Cos}^{2(1+2m)}\left\{ (1 + \frac{E_f^m}{U^m})\theta \right\} \qquad (14)$$

with half-width

$$\theta_w = \frac{\mathrm{Cos}^{-1}\ (\frac{1}{2})^{\frac{1}{2(1+2m)}}}{1 + (\frac{E_f}{U})^m} \ . \qquad (15)$$

This result shows the dependence of $S(\theta)$ and θ_w on the ratio of E_f/U and the value of m. Using the least square method to fit Equation (10) to the focusing parameter derived by Duesing and Leibfried (1965), the value of m was found to be equal to 0.485 if Abrahamson's parameters in Born-Mayer potential were used and equal to 0.404 if Anderson and Sigmund's parameters were used. Several values of θ_w are shown in Table III. The influence of m and E_f/U on $S(\theta)$ is shown in Figure 11. In general, the smaller the value of m, the wider the spread of the distribution. On the other hand, the sharpness of the distribution increases as the value of E_f/U increases. The value of E_f^{110} for nickel can be estimated by substituting $\theta_w = 8.5^o$ into Equation (15) and was found approximately equal to 68±22 eV, with U = 5.11 eV.

It was mentioned by Lenskjaer et al. (1974) that assuming the energy distribution of subsurface atoms to be collimated around the [110] direction and have the form

TABLE III. DEPENDENCE OF HALF-WIDTH θ_w ON m AND E_f/U

θ_w(Degrees)	m	
E_f/U	0.404	0.485
0.00	34.350	33.000
4.00	12.490	11.150
4.94	11.820	
29.54		5.350
40.00	6.32	4.730

TABLE IV. SURFACE BINDING AND SPUTTERING THRESHOLD ENERGIES FOR Ni.

Crystal surfaces	(110)	(100)	(111)
U (eV/atom)	5.11	5.55	5.61
Nearest-neighbors	7	8	9
Next-nearest-neighbors	4	5	3
E_T (eV) [110]	5.38	9.10	7.77

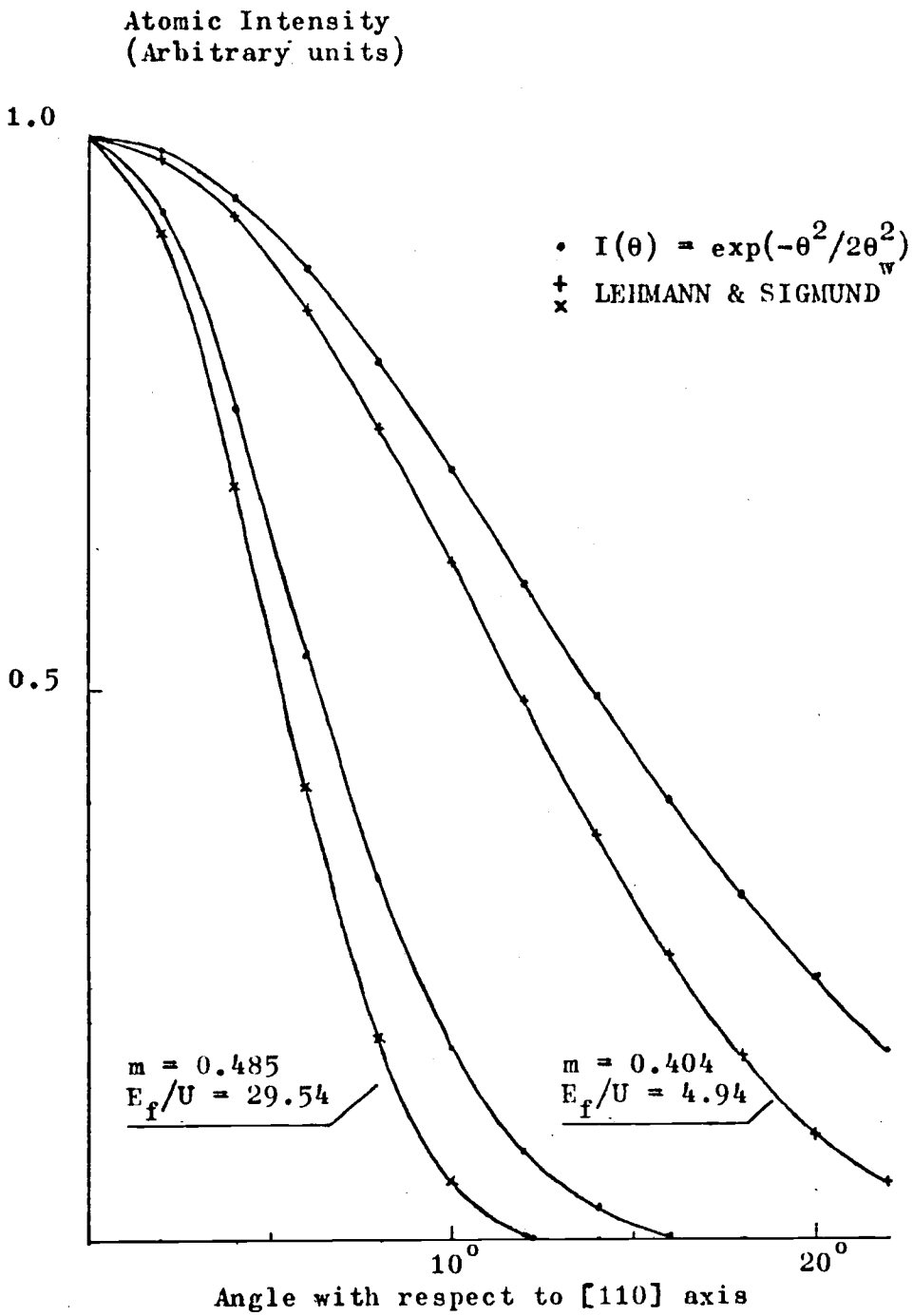

Figure 11. Angular distribution of surface atoms ejected near 110 axis from a f.c.c. crystal.

$$g(E_1,\theta_1) \sim E_1^{-2} \exp(-\theta_1^2/2\theta_w^2)$$

where θ_{1w} is the width of the distribution, the half-width θ_w was found to be in good agreement with experiment. Using $\theta_{1w} = 10^0$, the half-width of the <110> peak was reduced by a factor of $\frac{1}{2}$. They suggested that if the width θ_{1w} was determined by focused collision sequences, the last collision in such a sequence leading to the ejection of target atom might sharpen the angular distribution of ejected atoms substantially.

As Thompson (1968) pointed out that if focused collision sequences led to the ejection of atoms near the close-packed directions, a narrower range of angles and smaller spots in the ejection patterns could be expected. To determine the width θ_{1w}, he suggested to use the mean square angle of deviation given by Equation 11 or 12 and average it over the energy spectrum of the ejected atoms.

D. Low Energy Sputtering Yield

By assuming that cascades of atomic collisions induced sputtering, Sigmund (1969) developed an intergrodifferential equation for sputtering yield of amorphous and polycrystalline targets from the general Boltzman transport equation. For ion energy E less than E^* defined by

$$E^* = 0.023 \frac{M_1+M_2}{M_2} \frac{Z_1 Z_2}{Z_1^{2/3} + Z_2^{2/3}} \left(\frac{a_B}{a}\right)^2 \frac{e^2}{a} \qquad (16)$$

where M_1, M_2 and Z_1, Z_2 are the mass numbers and atomic numbers of the bombarding ion and target respectively, a_B is the Bohr radius, the sputtering yield at perpendicular incidence was found to be

$$S(E) = 0.304\ b \frac{M_1 M_2}{(M_1+M_2)^2} \frac{E}{U} \qquad (17)$$

where b is a constant depending on the mass ratio M_2/M_1. Apart from the mass numbers M_1 and M_2, Equation 17 shows that the low ion energy sputtering yield depends on the surface binding energy U, and especially linearly on the ion energy E. From the experimental work of Wehner and his group (Behrisch, 1964), experimental yield curves are indeed linear at energies from E^* down to somewhat below 100 eV, especially for not-too-light ions where E^* is not too small. For Ar^+-Ni sputtering experiment, according to Sigmund's theory, a linear yield curve should be expected at energies below 220 eV if a is chosen to be 0.28 Å or 460 eV if a is chosen to be 0.22 Å. For both cases, b = 0.3.

For single crystal sputtering, Sigmund suggested that only some modifications were needed to add to the theory of amorphous and polycrystalline target sputtering in order to describe the dominant effects of the regular lattice structure in single

crystal sputtering. The anisotrophy of atomic ejection from a single crystal was accounted for by a reduction of ion energy deposited near the crystal surface when ion bombardment was directed along a channeling direction.

In the single crystal sputtering theory of Onderdelinden (1966), based on Lindhard's theory of channeling (1965), the incident ion beam is thought of as being split into two parts: one part aligning with one of the open channels of the crystal and resulting in no sputtering, the other part moving randomly through the crystal and producing the same sputtering effect as if it were moving in a polycrystalline target of the same substance. Onderdelinden derived the following expression for single crystal sputtering yield

$$S_{(hkl)}(E, \varphi) = \frac{\epsilon_{hkl} P_{hkl}(E, \varphi) S_{poly.}(E)}{\cos \varphi}, \qquad (18)$$

where E is the ion energy, φ is the incident angle of ion making with the (hkl) surface normal, $S_{poly.}$ is the sputtering yield of the polycrystalline target, P_{hkl} is the probability of an ion entering the random part of the ion beam and ϵ_{hkl} is an efficency factor accounting for any orientation dependence of the sputtering mechanism.

The probability P_{hkl} is calculated from Lindhard's theory, which is based, in turn, on his approximate treatment of the scattering of particles which interact according to a Thomas-

Fermi potential, and is given by

$$P_{hkl}(E,\psi) = \left\{ \frac{p_o^2}{p_m^2(0)} + \left(1 - \frac{p_o^2}{p_m^2(0)}\right) \frac{\psi^2}{(C\psi_2)^2} \right\}^{-1} \qquad (19)$$

for $\psi < C\psi_2$ where ψ is the angle of the incident ion beam making with respect to a channel axis and $1 < C < 2$, and

$$p_o^2 = (\pi nd)^{-1}$$

where n is the atomic density of the target and d is the separation between two adjacent atoms along the axis,

$$p_m(0) = \psi_2 d$$

which is the minimum distance from the channel axis in which an ion, moving parallel to that direction, can enter the aligned beam, and

$$\psi_2 = \left\{ 2.350 \frac{Z_1 Z_2}{Z_1^{2/3} + Z_2^{2/3}} \left(\frac{a_B}{d}\right)^2 \frac{e^2}{Ed} \right\}^{\frac{1}{4}} . \qquad (20)$$

Onderdelinden found out that, the half-widths of minima in the [100], [211], and [411] directions appeared in the sputtering yield curves which were obtained by rotating a (100) copper crystal about a [011] axis and bombarding it with 5 - 35 keV argon ions were approximately proportional to $E^{-\frac{1}{4}}$ and in good agreement with the values of ψ_2 given by Equation (20), and concluded

that channeling of ion showed influence on the single crystal sputtering phenomenon.

Onderdelinden's model has been applied to explain the experimental sputtering yields of single gold and aluminum crystals, quite satisfactorily, to ion energy as low as 5 keV by Robinson and Southern (1967). At sufficiently low ion energy, Lindhard pointed out already that Equation (20) might overestimate the angle ψ_2, and also overlap of atoms in the neighboring rows may occur, corrections must be made to Onderdelinden's theory before it can be applied to low energy single crystal sputtering.

E. Sputtering Thresholds

The minimum energy for sputtering (threshold energy) is a very important physical quantity in deriving the information related to the atomic collision process near a target surface and in studying the atomic ejection mechanism. Even in the most efficient collision sequences, ions with this primary energy can only transfer an energy to a target atom equal to the surface binding energy of the target and cause the latter to be ejected.

All low energy single crystal sputtering experiments show the preferential ejection of target atoms in directions corresponding to the close-packed crystallographic directions of the target. The ejection patterns persist to the lowest bombarding ion energies.

Harrison and Magnuson (1961) developed a sputtering threshold theory based upon the Silsbee effect by assuming that, a surface atom, which was in turn an end member of a focused collision chain, could be ejected from a target if it acquired a certain amount of energy equal to or higher than the surface binding energy of the target. For mass ratio $\mu = M_1/M_2 < 1$, they derived an expression for the single crystal sputtering threshold energy, along a direction at an angle θ with respect to the normal of a (hkl) crystal surface

$$E_T(\theta) = \frac{U_{hkl}}{T_m}\left\{1 - \tfrac{1}{2}T_m\left[1 + \mu\,\mathrm{Sin}^2\theta - \mathrm{Cos}\,\theta\,(1 - \mu^2\mathrm{Sin}^2\theta)^{\frac{1}{2}}\right]\right\}^{-1}$$

with $T_m = 4M_1M_2/(M_1 + M_2)^2$, and U_{hkl} is the atomic surface binding energy of the crystal.

By using a Morse potential for the (100), (110) and (111) surfaces of cubic crystals and assuming that the atomic planes were true planes, i.e. there is no atom protruding above or below the planes, and including the surface relaxation effects, Jackson (1973) showed a comprehensive calculation of the surface binding energies. For f.c.c. metals, his results show the following trend of surface binding energies: $U_{110} \lesssim U_{100} \lesssim U_{111}$, which is in the reverse of the order of the surface relaxations. The surface binding energies calculated by Jackson and the sputtering threshold energies along the [110] directions, obtained by substituting Jackson's surface binding energies into Harrison

and Magnuson's equation, for the (110), (100) and (111) nickel crystals are listed in Table IV. The Harrison-Magnuson theory predicts a threshold value of 5.4 eV for ejecting nickel atoms along the [110] direction from a (110) crystal, and a threshold value of 7.8 eV from a (111) crystal. The most probable threshold energy required to eject nickel atoms along the [110] direction from a (110) nickel crystal obtained in this work was 10 eV, while for a (111) nickel crystal the threshold appeared to have a value of about 15 eV. The higher experimental thresholds than the theoretical predictions may indicate that the collision model coupled with the chaining mechanism used by Harrison and Magnuson is too simple to explain the sputtering threshold satisfactorily.

V. CONCLUSIONS

Low energy single crystal sputtering provides information for atomic collision and ejection processes near a target surface. While the theory for explaining this phenomenon is still in the developing stage, improvements in experimental technique and results will enlarge the understanding of the collision and ejection mechanisms and help to improve the theory of sputtering. Sputtering experiments furnished the evidence of directional phenomenon, i.e. ejection of atoms from a target, especially along the close-packed direction in a single crystal, and led to the development of Silsbee's focused collision sequences.

The results of this work clearly and strongly exhibit the ejection of atoms along the close-packed crystal direction in a f.c.c. crystal as the angular distributions of nickel atoms, whether they were ejected from a (110) or a (111) nickel crystal, peak at angles corresponding to the [110] direction or others belonging to the same category. The amount of nickel atoms ejected as a result of ion bombardment with energy less than 600 eV was small. Radioactive tracing technique shows the advantage over other techniques because it is sensitive to such small number of radioactive atoms hence the sputtering experiment does not require a large dose of ions or a lengthy bombardment which could result in contamination on or damage to the target surface.

In low energy single crystal sputtering, the binding energy of a crystal surface may be a dominant factor in the atomic ejection process. At the same ion energy and ejection along a [110] direction, the sputtering yield was found higher from a (110) crystal than that from a (111) crystal.

The half-widths of <110> peaks in the ejection patterns of nickel atoms obtained from nickel single crystals bombarding with low energy argon ions were found to be independent of the ion energy, or to be insignificant at least, up to an argon ion energy of 600 eV, as they all showed an extent of about 8.5^{o}. The half-width of a <110> peak may depend on the focusing energy E_f^{110}, surface binding energy and atomic mass of the target, as suggested by Lehmann and Sigmund.

In Lehmann and Sigmund's model of single crystal sputtering, the appearance of <110> spot is explained by using the fact that atoms lying along the [110] direction experience the lowest binding energy hence can be ejected from the crystal easier than those lying along other directions. On the other hand, in the focuson model of single crystal sputtering, the development of a sequence of focused collisions is required before the end member of this chain which is located at the crystal surface and receives sufficient energy to overcome the surface binding energy of the crystal can be ejected. Recently, Lenskjaer et al. (1974) linked the focuson to the Lehmann and Sigmund's theory because such connection gave a half-width of the <110> peak in good

agreement with experiment. This approach, at the present time, seems quite acceptable.

The experimental threshold energy required to eject nickel atoms along the [110] direction from a (110) nickel crystal as a result of low energy argon ion bombardment was estimated to be 10 eV. For a (111) nickel crystal, the threshold energy appeared to have a value of about 15 eV. These results provide a rough estimate of the sputtering thresholds for nickel single crystals under low energy argon ion bombardment. Further work is still required before the final values of threshold energies can be claimed.

BIBLIOGRAPHY

1. Abrahamson, A. A. Born-Mayer-type interatomic potential for neutral ground-state atoms with Z=2 to Z=105. Physical Review 178: 76-79. February 1969.

2. Andersen, H. H. and Sigmund, P. Deffect distributions in channeling experiments. Nuclear Instruments and Methods 38: 238-240. June 1965.

3. Askerov, S. G. and Sena, L. A. Cathode sputtering of metals by slow mercury ions. Soviet Physics-Solid State 11: 1288-1293. December 1969.

4. Behrisch, R. Festkörperzerstäubung durch ionenbeschuβ. Ergebnisse der Exackten Naturwissenschaften 35: 295-443. 1964.

5. Chadderton, L. T. et al. A contribution to sputtered ejection patterns from collision sequences in atomic ejection cascades: firm evidence from channeling experiments. Radiation Effects 13: 75-80. March 1972.

6. Chapman, G. E. and Kelly, J. C. The angular distribution of atoms sputtered from monocrystalline gold. Australian Journal of Physics 20: 283-289. June 1967.

7. Cuderman, J. F. and Brady, J. J. Relative sputtering yields from close-packed directions in nickel under low-energy Ar^+ bombardment. Surface Science 10: 410-418. June 1968.

8. Duesing, G. and Leibfried, G. Fokussierende stoβfolgen in flächensentrierten kristallen und ihre bedeutung für verschiedene bestrahlungseffekte. Physica Status Solidi 9: 463-484. May 1965.

9. Endzheets, G. et al. Angular distribution of particles scattered as a result of irradiation of monocrystals with ionic beams. Soviet Physics-Technical Physics 7: 752-753. February 1963.

10. Farmery, B. W. and Thompson, M. W. Energy spectra for copper. Philosophical Magazine 18: 415-424. August 1968.

11. Gibson, J. B., Goland, A. N., Milgram, M. and Vineyard, G. H. Dynamics of radiation damage. Physical Review 120: 1229-1253. November 1960.

12. Grove, W. R. On the electro-chemical polarity of gases. Philosophical Transactions of The Royal Society of London 142: 87-90. 1852.

13. Harrison, D. E., Johnson, J. P. and Levy, N. S. Spot patterns and Silsbee chains on Cu single crystal. Applied Physics Letters 8: 33-36. January 1966.

14. Harrison, D. E. and Magnuson, G. D. Sputtering Thresholds. Physical Review 122: 1421-1430. June 1961.

15. Hoffer, W. O. Distribution of sputtering spot patterns of single crystals due to incomplete condensation. Radiation Effects 21: 141-143. March 1974.

16. Jackson, D. P. Binding energies in cubic metal surfaces. Radiation Effects 18: 185-189. April 1973.

17. Kanaya, K. et al. Consistent theory of sputtering of solid targets by ion bombardment using power potential law. Japaness Journal of Applied Physics 30: 1388-1396. September 1973.

18. Lehmann, C. and Sigmund, P. On the mechanism of sputtering. Physica Status Solidi 16: 507-511. August 1966.

19. Leibfried, G. Correlated collisions in a displacement spike. Journal of Applied Physics 30: 1388-1396. September 1959.

20. Lenskjaer, T. et al. A note on ejection of surface atoms in single crystal sputtering. Physics Letters 47A: 63-65. February 1974.

21. Lindhard, J. Influence of crystal lattice on motion of energetic charged particles. Matematisk-Fysiske Meddelser udgivet af Det Kongelige Danske Videnskabernes Selskab 34: No. 14. 1965.

22. Nelson, R. S. and Thompson, M. W. Atomic collision sequences in crystals of copper, silver and gold revealing by sputtering in energetic ion beams. Proceedings of The Royal Society of London 259A: 458-481. January 1961.

23. Nelson, R. S., Thompson, M. W. and Montgomery, H. The influence of thermal vibration on focused collision sequences. Philosophical Magazine 7: 1385-1405. May 1962.

24. Nelson, R. S. Randomisation of crystal structure within energetic collision cascades revealed by the sputtering of Au single crystals during ion bombardment. Radiation Effects 7: 263-267. February 1971.

25. Oechsner, H. Energy distribution in sputtering process. Physical Review Letters 24: 583-584. March 1970.

26. Onderdelinden, D. The influence of channeling on Cu single crystal sputtering. Applied Physics Letters 8: 189-190. April 1966.

27. _____. Single-crystal sputtering including the channeling phenomenon. Canadian Journal of Physics 46: 739-745. March 1968.

28. Pleshivtsev, N. V. The technology of cathode sputtering. Instrument and Experimental Techniques 5: 929-957. April 1965.

29. Robinson, M. T. and Southern, A. L. Sputtering experiments with 1- to 5-keV Ar^+ ions. II. Monocrystalline targets of Al, Cu and Au. Journal of Applied Physics 38: 2969-2973. June 1967.

30. Sigmund, P. Theory of sputtering. I. Sputtering yield of amorphous and polycrystalline targets. Physical Review 184: 383-415. April 1969.

31. Silsbee, R. H. Focusing in collision problems in solids. Journal of Applied Physics 28: 1246-1250. November 1957.

32. Stuart, R. V. and Wehner, G. K. Sputtering yields at very low energies. Journal of Applied Physics 33: 2345-2352. July 1962.

33. Thompson, M. W. The energy spectrum of ejected atoms during the high energy sputtering of gold. Philosophical Magazine 18: 377-414. August 1968.

34. _____. Defects and Radiation Damage in Metals. London, Cambridge U. P. 1969. 384p.

35. Verma, S. K. and Wilman, H. Epitaxy and oblique face development in nickel electrodeposits on a copper cube face in relation to rate of deposition, deposit thickness, degree of stirring and bath temperature. Journal of Physics D: Applied Physics 4: 1167-1175. August 1971.

36. Wehner, G. K. Sputtering of metal single crystals by ion bombardment. Journal of Applied Physics 26: 1056-1057. August 1955.